Supporting Information

Kimber et al. 10.1073/pnas.1318543111

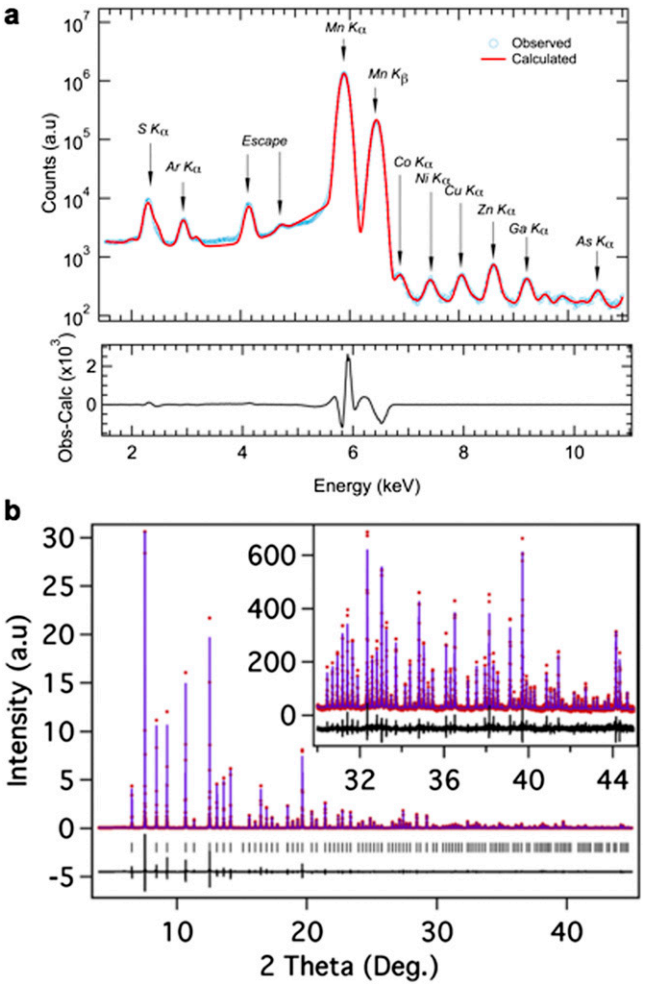

Fig. S1. Characterization of sample purity and ambient pressure structure. (*A*) X-ray fluorescence measurements showed the presence of minor transition metal impurities at a level of less than 0.1%. Similar levels of Se and As contamination were observed. The model calculation was performed using the PyMca software from the European Synchrotron Radiation Facility (ESRF). (*B*) Very high-resolution powder X-ray diffraction data collected at 55 K on ID31 at the ESRF showed no deviation from the cubic $Pa\bar{3}$ pyrite structure, and no evidence for significant impurities. The refinement shown below converged with $\chi^2 = 5.38$ and gave a refined lattice parameter a = 6.088821(4) Å and a refined sulfur coordinate of x = 0.400061(6).

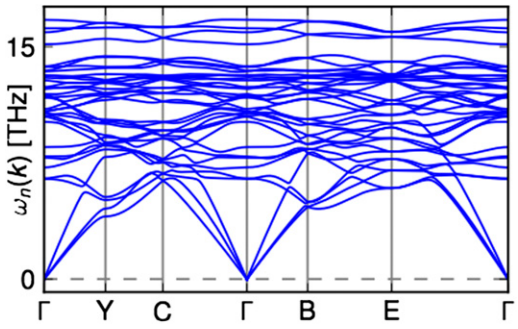

Fig. S2. Phonon dispersion of the high-pressure polymorph of MnS_2at 20 GPa. We investigated the stability of our high-pressure structure by calculating the phonon band structure. All frequencies are real. The high symmetry points of the monoclinic $P\,2_1/c$ structure are $Y = (\frac{1}{2},0,0)$, $C = (\frac{1}{2},\frac{1}{2},0)$, $B = (0,0,\frac{1}{2})$, and $E = (\frac{1}{2},\frac{1}{2},\frac{1}{2})$.

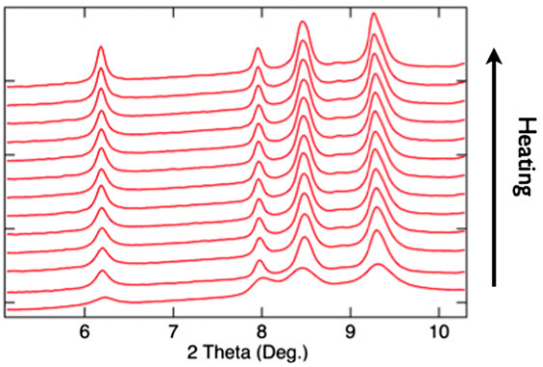

Fig. S3. Diffraction data during in situ laser heating of MnS_2. Data are shown immediately after commencing laser heating. The frame rate was ~1 Hz, and the highest temperature reached was ~1,800 K, as judged by thermal emission.

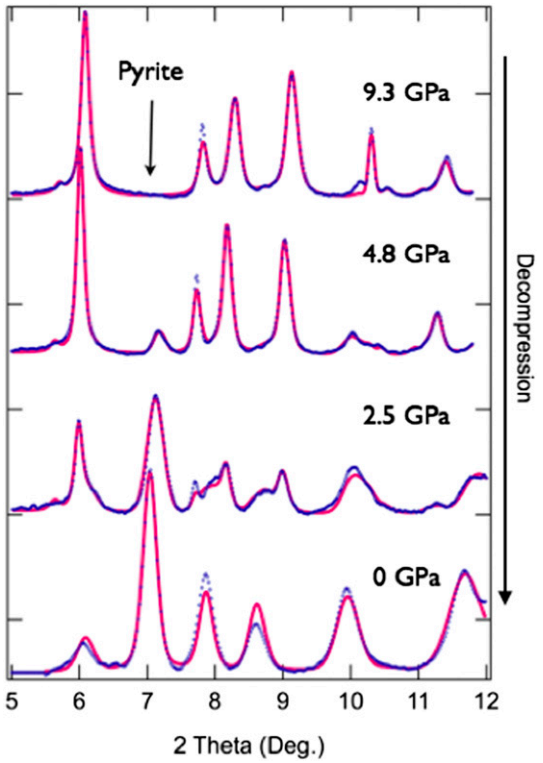

Fig. S4. Diffraction data collected during the decompression of MnS_2. The diffraction data shown below were collected on decompressing the sample that had been laser heated. The dots are data points and the lines are model calculations using the arsenopyrite/pyrite structure models as appropriate. Note the onset of mixed phase behavior below ~ 5 GPa and the recovery of the pyrite phase.

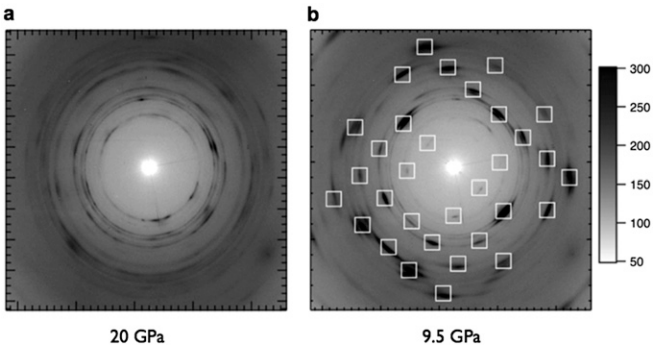

Fig. S5. Texture effects on decompression. Raw diffraction images are shown for the ID9 data at the highest pressure (30 GPa), and after reducing pressure to 9.5 GPa. We discovered that strong texturing sets in on decompression as highlighted by the white squares in *B*.

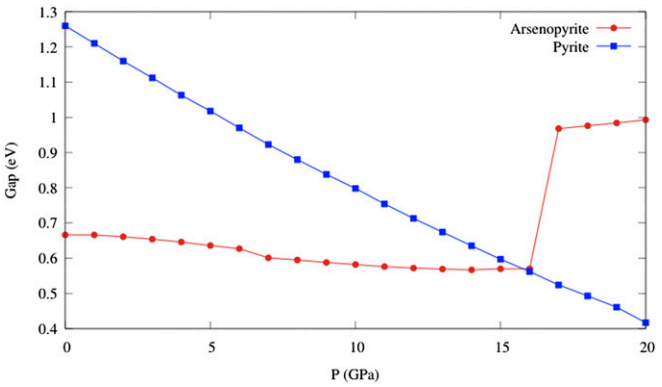

Fig. S6. Pressure dependence of the band gaps in pyrite and arsenopyrite MnS_2. The pressure dependence of the band gaps calculated using the LAPW method for both phases of MnS_2 is shown. Note the increase in the band gap of the arsenopyrite phase at 16 GPa, where the Mn–Mn dimerization is enhanced.

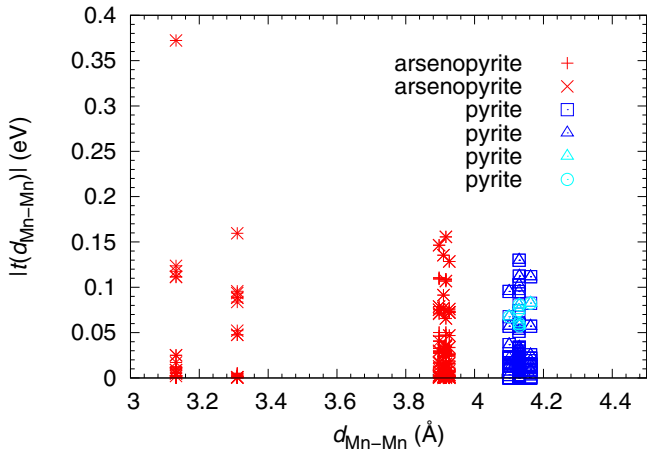

Fig. S7. Results of tight-binding fits to the electronic structure of pyrite and arsenopyrite MnS_2. Tight-binding parameter values for the 20 Mn *3* bands in the pyrite and arsenopyrite structures at $P = 10$ GPa, as obtained from projective Wannier functions within the full potential local orbital basis. One especially large hopping parameter for the shortest Mn–Mn bond appears in the arsenopyrite structure. It corresponds to a $3d_{xz}$–$3d_{xz}$ Wannier function overlap.

Table S1. Arsenopyrite structures of MnS_2 from $P = 10$ GPa to $P = 20$ GPa

Mn x	Mn y	Mn z	S(1) x	S(1) y	S(1) z	S(2) x	S(2) y	S(2) z
$P = 10$ GPa, space group $P\,2_1/c$, $a = 5.59345$ Å, $b = 5.47203$ Å, $c = 5.58484$ Å, $\beta = 109.920°$								
−0.25112	−0.00017	−0.25197	−0.34402	0.37298	−0.15687	−0.15568	−0.37358	−0.34563
$P = 11$ GPa, space group $P\,2_1/c$, $a = 5.57405$ Å, $b = 5.46472$ Å, $c = 5.57233$ Å, $\beta = 109.965°$								
−0.25316	0.49971	−0.25569	−0.34380	−0.12766	−0.15920	−0.15530	0.12619	−0.34785
$P = 12$ GPa, space group $P\,2_1/c$, $a = 5.55490$ Å, $b = 5.45567$ Å, $c = 5.56002$ Å, $\beta = 110.171°$								
−0.25700	0.49947	−0.26255	−0.34304	−0.12850	−0.16333	−0.15490	0.12538	−0.35198
$P = 13$ GPa, space group $P\,2_1/c$, $a = 5.54785$ Å, $b = 5.45037$ Å, $c = 5.55599$ Å, $\beta = 109.960°$								
−0.25616	−0.00053	−0.26113	−0.34320	0.37155	−0.16257	−0.15492	−0.37429	−0.35132
$P = 14$ GPa, space group $P\,2_1/c$, $a = 5.53365$ Å, $b = 5.44896$ Å, $c = 5.54880$ Å, $\beta = 110.396°$								
−0.25912	0.49923	−0.26632	−0.34242	−0.12912	−0.16642	−0.15494	0.12537	−0.35440
$P = 15$ GPa, space group $P\,2_1/c$, $a = 5.46505$ Å, $b = 5.42287$ Å, $c = 5.50583$ Å, $\beta = 111.581°$								
−0.27172	0.00018	−0.28596	−0.34104	0.36922	−0.17620	−0.15378	−0.37473	−0.36770
$P = 16$ GPa, space group $P\,2_1/c$, $a = 5.46440$ Å, $P = 18$ GPa, $c = 5.49656$ Å, $\beta = 111.442°$								
−0.27002	0.00028	−0.28314	−0.34156	0.36888	−0.17483	−0.15350	−0.37510	−0.36454
$P = 17$ GPa, space group $P\,2_1/c$, $a = 5.43310$ Å, $b = 5.40310$ Å, $c = 5.48509$ Å, $\beta = 111.833°$								
−0.27380	0.00029	−0.28821	−0.34148	0.36845	−0.17739	−0.15302	−0.37532	−0.36762
$P = 18$ GPa, space group $P\,2_1/c$, $a = 5.42415$ Å, $b = 5.39539$ Å, $c = 5.47696$ Å, $\beta = 111.869°$								
−0.27388	−0.49972	−0.28839	−0.34134	−0.13157	−0.17760	−0.15306	0.12472	−0.36771
$P = 19$ GPa, space group $P\,2_1/c$, $a = 5.41550$ Å, $b = 5.38817$ Å, $c = 5.46917$ Å, $\beta = 111.888°$								
−0.27380	0.00024	−0.28843	−0.34118	0.36844	−0.17775	−0.15312	−0.37524	−0.36779
$P = 20$ GPa, space group $P\,2_1/c$, $a = 5.40735$ Å, $b = 5.38104$ Å, $c = 5.46141$ Å, $\beta = 111.912°$								
−0.27380	0.00020	−0.28848	−0.34108	0.36845	−0.17792	−0.15312	−0.37522	−0.36777

Table S2. Refined pyrite and arsenopyrite structures of MnS_2 at $P = 0$ and 20 GPa respectively

Mn x	Mn y	Mn z	S(1) x	S(1) y	S(1) z	S(2) x	S(2) y	S(2) z
$P = 0$ GPa, space group $Pa-3$, $a = 6.0888214(5)$, S(x)=0.400061(6) Å								
$P = 20$ GPa, space group $P\,2_1/c$, $a = 5.4642(6)$ Å, $b = 5.3742(5)$ Å, $c = 5.4203(7)$ Å, $\beta = 111.93(2)°$								
0.280(2)	0.012(2)	0.288(1)	0.345(2)	0.375(2)	0.175(2)	−0.139(2)	0.601(2)	−0.368(2)

In the pyrite structure, the Mn atoms are on the *4a* position, and the S atoms are on the *8c* position. The pyrite density is 4.85 g/cm^3. In the arsenopyrite structure, the Mn atoms, and the two independent S sites are on the *4e* position. The arsenopyrite density is 6.385 g/cm^3.